Influence of the dba Substitution on the Reactivity of Palladium(0) Complexes Generated from Pd^0_2(dba-*n,n′*-Z)$_3$ or Pd^0(dba-*n,n′*-Z)$_2$ and PPh_3 in Oxidative Addition with Iodobenzene

Yohan Macé,† Anant R. Kapdi,‡ Ian J. S. Fairlamb,*,‡ and Anny Jutand*,†

Département de Chimie, Ecole Normale Supérieure, UMR CNRS-ENS-UPMC 8640, 24, Rue Lhomond. F-75231 Paris Cedex 5, France, and Department of Chemistry, University of York, Heslington, York YO10 5DD, U.K.

Received December 22, 2005

The reactivity of Pd(0) complexes generated by addition of PPh_3 (PPh_3/Pd = 2, 4) to either Pd^0_2(dba-*n,n′*-Z)$_3$ (*n,n′*-Z = 4,4′-F, 4,4′-H, 4,4′-MeO, 3,3′,4,4′,5,5′-OMe) or Pd^0(dba-*n,n′*-Z)$_2$ (*n,n′*-Z = 4,4′-Br, 4,4′-Cl, 4,4′-H, 4,4′-CH_3, 3,3′,5,5′-OMe) in DMF is affected by the electron-donating or -accepting properties of the groups Z substituted on the aromatic rings of dba. Whatever the nature of Z, the unreactive major complexes $Pd^0(\eta^2$-dba-*n,n′*-Z)$(PPh_3)_2$ are formed, which are in equilibrium with the common reactive complex $Pd^0(PPh_3)_2$ and dba-*n,n′*-Z. The latter controls the concentration of the reactive $Pd^0(PPh_3)_2$ and, consequently, also controls the rate of the overall oxidative addition with phenyl iodide. The more electron donating the Z group, the lower the affinity of dba-4,4′-Z for $Pd^0(PPh_3)_2$. As a result, the overall rate of the oxidative addition with PhI is faster when Z is an electron-donating group. For a given Z, the overall oxidative addition is faster when using Pd^0_2(dba-*n,n′*-Z)$_3$ instead of Pd^0(dba-*n,n′*-Z)$_2$. Therefore, the rate of the oxidative addition can be modulated by changing the electronic properties of the dba ligands determined by substituents on its phenyl groups and by changing the structure of the precursors: Pd^0_2-(dba-*n,n′*-Z)$_3$ versus Pd^0(dba-*n,n′*-Z)$_2$.

Introduction

It has been established that the coordination of Pd^0L_2 (L = phosphine, arsine) complexes by alkenes,[1,2] alkynes,[1,3] or vinyltin derivatives,[1,4] which are reagents in palladium-catalyzed Heck, Sonogashira, and Stille coupling processes, respectively, strongly affects the kinetics of the oxidative addition to aryl halides, which is the first step of their catalytic cycles (Scheme 1). Indeed, the complexation of the active Pd^0L_2 complex to form the unreactive complexes (η^2-CH_2=CHR)Pd^0L_2 or (η^2-CH≡CR)Pd^0L_2 results in slower oxidative additions by decreasing the concentration of the active Pd^0L_2 complex (Scheme 1).

It was recently reported that (η^2-alkene)Pd^0(iminophosphine)-catalyzed Suzuki−Miyaura reactions resulted in higher reaction rates when the alkene is a moderate π-accepting ligand.[5] This is explained by a stabilization of the active Pd^0(iminophosphine) complex by the alkene, thus preventing its decomposition to palladium black.

$Pd^0_2(dba)_3$ or $Pd^0(dba)_2$ (dba = *trans,trans*-dibenzylideneacetone), associated with ligands L (triarylphosphines), are often employed as sources of Pd^0 complexes in palladium-catalyzed reactions (Heck, Stille, Tsuji-Trost, etc.). It has been established by Amatore, Jutand, et al. that the presumably "innocent" dba ligand delivered by the precursor $Pd^0(dba)_2$ in reality plays a significant role in catalysis via alkene ligation to the active Pd^0L_2 complexes to generate $Pd^0(dba)L_2$ complexes (Scheme 2).[6−9] The presence of the dba ligand has a great consequence on the kinetics of oxidative additions with aryl halides, since dba controls the concentration and then the reactivity of the active species Pd^0L_2 (Scheme 3).[6−8] Indeed, Pd^0L_2 is always generated at low concentration, due to its unfavorable equilibrium with $Pd^0(dba)L_2$, the major but unreactive species (Scheme 3).[6−8]

It has been reported by Fairlamb et al. that the efficiency of palladium-catalyzed Suzuki-Miyaura cross-coupling of aryl

Scheme 1

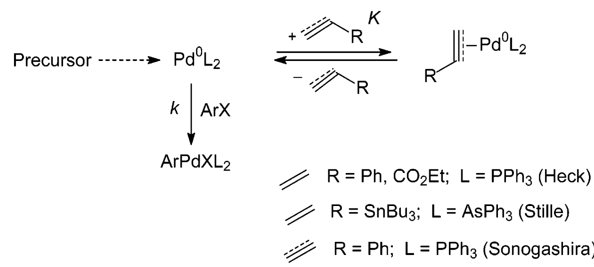

Scheme 2

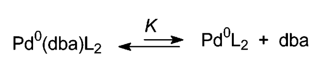

* To whom correspondence should be addressed. Fax: 33 1 4432 3325 (A.J.). E-mail: Anny.Jutand@ens.fr (A.J.); ijsf1@york.ac.uk (I.J.S.F.).
† Ecole Normale Supérieure.
‡ University of York.

(1) Jutand, A. *Pure Appl. Chem.* **2004**, *76*, 565−576.
(2) Amatore, C.; Carré, E.; Jutand, A.; Medjour, Y. *Organometallics* **2002**, *21*, 4540−4545.
(3) Amatore, C.; Bensalem. S.; Ghalem, S.; Jutand, A.; Medjour, Y. *Eur. J. Org. Chem.* **2004**, 366−371.
(4) Amatore, C.; Bucaille, A.; Fuxa, A.; Jutand, A.; Meyer, G.; Ndedi Ntepe, A. *Chem. Eur. J.* **2001**, *7*, 2134−2142.
(5) (a) Scrivanti, A.; Beghetto, V.; Matteoli, U.; Antonaroli, S.; Marini, A.; Mandoj, F.; Paolesse, R.; Crociani, B. *Tetrahedron Lett.* **2004**, *45*, 5861−5864. (b) Scrivanti, A.; Beghetto, V.; Matteoli, U.; Antonaroli, S.; Marini, A.; Crociani, B. *Tetrahedron* **2005**, *61*, 9752−9738.
(6) Amatore, C.; Jutand, A.; Khalil, F.; M'Barki, M. A.; L. Mottier, L. *Organometallics* **1993**, *12*, 3168−3178.
(7) Amatore, C.; Jutand, A.; Meyer, G. *Inorg. Chim. Acta* **1998**, *273*, 76−84.
(8) Amatore, C.; Jutand, A. *Coord. Chem. Rev.* **1998**, *178−180*, 511−528.
(9) Herrmann, W. A.; Thiel, W. R.; Brossmer, C.; Öfele, K.; Priermeier, T.; Scherer, W. *J. Organomet. Chem.* **1993**, *461*, 51−60.

10.1021/om0510876 CCC: $33.50
Publication on Web 03/03/2006

Table 1. Characterization of $Pd^0(\eta^2$-dba-*n*,*n*′-Z)$(PPh_3)_2$ Complexes by Cyclic Voltammetry[a] and NMR Spectroscopy[b] in DMF at 20 °C[c]

	n,*n*′-Z	$Pd^0(\eta^2$-dba-*n*,*n*′-Z)$(PPh_3)_2$ E^p_{ox} (V vs SCE)	^{31}P NMR: δ (ppm); $\Delta\nu_{1/2}$ (Hz)	^{19}F NMR: δ (ppm)
1	4,4′-CF_3		27.53 (s), 25.14 (s)	114.81 (s)
2	4,4′-Br	(+0.640)[c]	26.82 (s), 24.73 (s); 14	
3	4,4′-Cl	(+0.665)[c]	26.91 (s), 24.83 (s); 14	
4	4,4′−F	+0.630	26.93 (s), 24.65(s); 20	64.34 (s), 58.29 (s)
5	4,4′−H	+0.580 (0.600)[c]	26.79 (s), 24.97 (s); 23	
6	4,4′-Me	(0.570)[c]	26.35 (s), 24.99 (s); 33	
7	4,4′-OMe	+0.415	26.39 (s), 24.60 (s); 57	
8	3,3′,5,5′-OMe	(+0.575)[c]	26.94 (s), 25.21 (s); 19	
9	3,3′,4,4′,5,5′-OMe	+0.765	26.63 (s), 25.36 (s); 28	

[a] At a stationary-gold-disk electrode (diameter 2 mm) with a scan rate of 0.2 V s^{-1} in DMF (containing nBu_4NBF_4 0.3 M). [b] ^{31}P NMR (101.3 MHz, H_3PO_4) and ^{19}F NMR (235.3 MHz, $CFCl_3$) in DMF containing 10% acetone-d_6 for the lock. [c] $Pd^0(\eta^2$-dba-*n*,*n*′-Z)$(PPh_3)_2$ complexes are generated from Pd^0_2(dba-*n*,*n*′-Z$)_3$ or Pd^0(dba-*n*,*n*′-Z$)_2$ associated with 2 equiv of PPh_3/Pd. The oxidation potentials of Pd^0(dba-*n*,*n*′-Z)$(PPh_3)_2$ generated from Pd^0(dba-*n*,*n*′-Z$)_2$ are given in parentheses.

Scheme 3

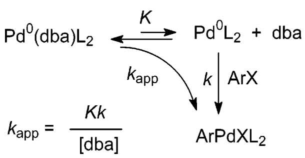

chlorides was strongly affected by the electronic properties of substituted dba-*n*,*n*′-Z when the precursor was Pd^0_2(dba-*n*,*n*′-

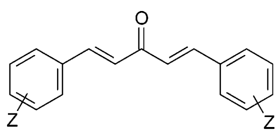

dba-n,n'-Z

Z$)_3$ associated with electron-rich ligands.[10] In the preliminary catalysis studies, it was established that a more electron-rich dba (i.e., substituted by electron-donating groups Z) favors higher yields of the cross-coupled product (an observation that is not substrate dependent). It was then of considerable interest to probe the influence of Z substitution of dba on the kinetics of oxidative additions to determine whether the effect observed in catalytic reactions took its origin in the oxidative-addition step, which is probably rate determining when aryl chlorides are considered.

We report herein that the kinetics of oxidative additions of phenyl iodide with the palladium(0) complexes generated from Pd^0_2(dba-*n*,*n*′-Z$)_3$ or Pd^0(dba-*n*,*n*′-Z$)_2$ associated with PPh_3 (taken as model ligand) are indeed affected by the electronic properties of dba, which are modulated by substituents Z on its phenyl groups.

Results and Discussion

Characterization of the Pd^0 Complexes Generated from Pd^0_2(dba-*n*,*n*′-Z$)_3$ or Pd^0(dba-*n*,*n*′-Z$)_2$ and PPh_3 (PPh_3/Pd = 2, 4) in DMF. Two kinds of precursors are available, Pd^0_2-(dba-*n*,*n*′-Z$)_3$ (*n*,*n*′-Z = 4,4′-F, 4,4′-H, 4,4′-MeO, 3,3′,4,4′,5,5′-OMe) and Pd^0(dba-*n*,*n*′-Z$)_2$ (*n*,*n*′-Z = 4,4′-CF_3, 4,4′-Br, 4,4′-Cl, 4,4′-H, 3,3′,5,5′-OMe), according to their ability to crystallize.[10,11] All precursors have been reacted with PPh_3 (2 equiv per Pd) in DMF, and the major complexes $Pd^0(\eta^2$-dba-*n*,*n*′-Z)$(PPh_3)_2$, formed in all reactions, have been characterized by ^{31}P NMR spectroscopy and cyclic voltammetry (Scheme 4, Table 1). The η^2-coordination of the substituted dba-*n*,*n*′-Z was supported by the detection of two different ^{31}P NMR signals, as observed for nonsubstituted dba.[6,8,9]

Scheme 4

$$^1/_2Pd^0(\text{dba-}n,n'\text{-Z})_3 + 2PPh_3 \rightarrow Pd^0(\eta^2\text{-dba-}n,n'\text{-Z})(PPh_3)_2 + {}^1/_2\text{dba-}n,n'\text{-Z}$$

$$Pd^0(\text{dba-}n,n'\text{-Z})_2 + 2PPh_3 \rightarrow Pd^0(\eta^2\text{-dba-}n,n'\text{-Z})(PPh_3)_2 + \text{dba-}n,n'\text{-Z}$$

The characterization of complexes generated from Pd^0_2(dba-4,4′-F$)_3$ associated with PPh_3 is reported here in detail and compared to the case for $Pd^0_2(dba)_3$. The behavior of the precursor $Pd^0_2(dba)_3{\cdot}CHCl_3$ associated with phosphines has indeed never been reported. When PPh_3 was added to Pd^0_2-(dba-4,4′-F$)_3$ (PPh_3/Pd = 2) in DMF (containing 10% acetone-d_6 for the lock), two broad singlets were observed in the ^{31}P NMR spectra, characterizing two different PPh_3 groups and attesting to the formation of $Pd^0(\eta^2$-dba-4,4′-F)$(PPh_3)_2$ in which the dba-4,4′-F ligand was coordinated to the Pd^0 center by one of its C═C bonds (Scheme 5), as classically observed for the simple nonsubstituted dba ligand.[6−9] The monocoordination of dba-4,4′-F was further confirmed by the ^{19}F NMR spectrum recorded from the same NMR tube, which exhibited three singlets. One sharp singlet at 66.26 ppm characterizes the free dba-4,4′-F (Figure 1, first equation in Scheme 5). The other two broader singlets of equal magnitude at 64.34 and 58.29 ppm characterized the unsymmetrical ligation of dba-4,4′-F, which results in the two magnetically different fluorine atoms F_a and F_b (Figure 1, Scheme 5).

After addition of PhI (10 equiv), only the ^{19}F NMR singlet of the free 4,4′-F-dba was observed as well as the ^{31}P NMR singlet of *trans*-PhPdI$(PPh_3)_2$ at 22.98 ppm, similar to that of

Scheme 5

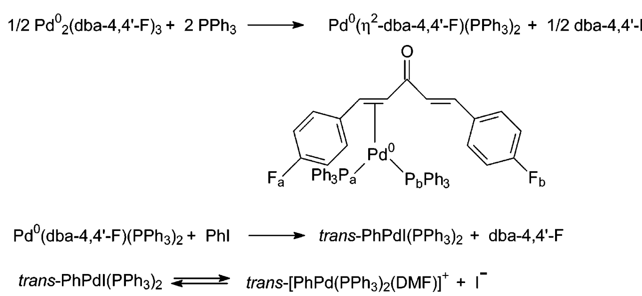

(10) Fairlamb, I. J. S.; Kapdi, A. R.; Lee, A. F. *Org. Lett.* **2004**, *6*, 4435−4438.
(11) Fairlamb, I. J. S.; Kapdi, A. R.; Whitwood, A. C. Manuscript in preparation.

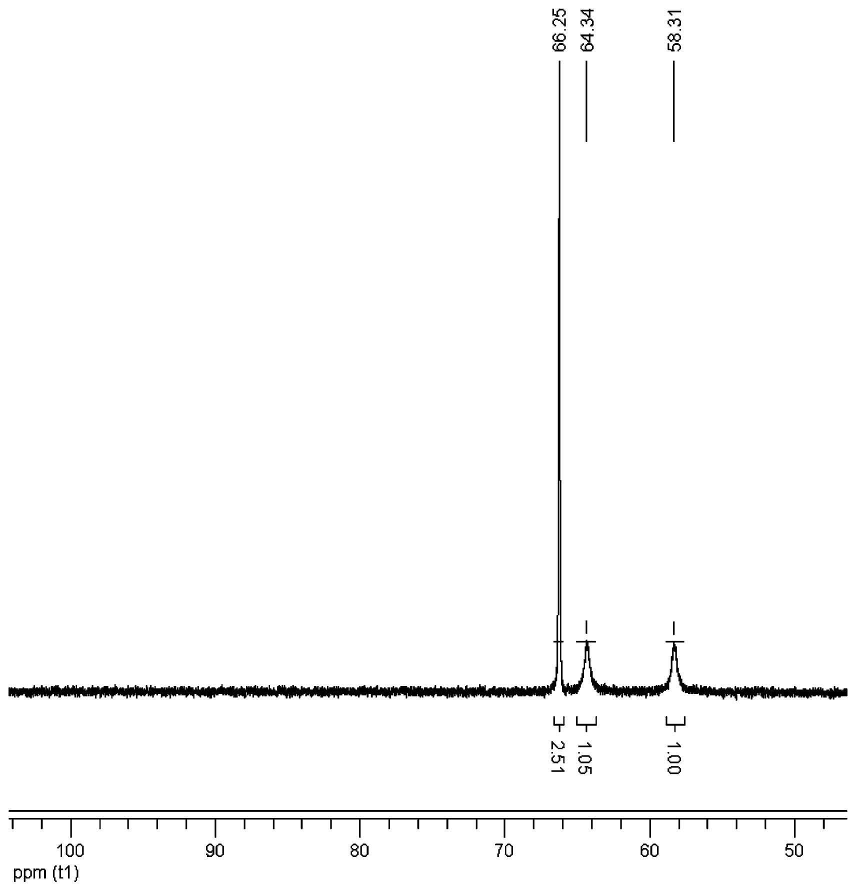

Figure 1. ^{19}F NMR (235.3 MHz, $CFCl_3$) spectrum of $Pd^0(\eta^2$-dba-4,4′-F)$(PPh_3)_2$ generated from Pd^0_2(dba-4,4′-F)$_3$ associated with 2 equiv of PPh_3/Pd in DMF containing 10% acetone-d_6.

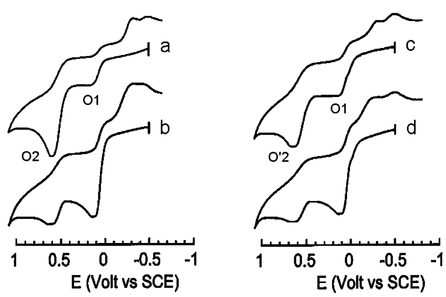

Figure 2. Cyclic voltammetry at a stationary-gold-disk electrode (diameter 2 mm) performed in DMF (containing nBu$_4$NBF$_4$ 0.3 M) with a scan rate of 0.2 V s^{-1}, at 20 °C: (a) $Pd^0_2(dba)_3$ (1 mM) + PPh_3 (4 mM); (b) $Pd^0_2(dba)_3$ (1 mM) + PPh_3 (8 mM); (c) Pd^0_2-(dba-4,4′-F)$_3$ (1 mM) + PPh_3 (4 mM); (d) Pd^0_2(dba-4,4′-F)$_3$ (1 mM) + PPh_3 (8 mM).

an authentic sample. A second minor singlet was also observed at 20.86 ppm, which characterizes the cationic complex *trans*-$[PhPd(PPh_3)_2(DMF)]^+$ in equilibrium with *trans*-$PhPdI(PPh_3)_2$[12] (last equation in Scheme 5). The spectroscopic data indicate that a definite oxidative addition reaction with PhI took place.

When PPh_3 was added to $Pd^0_2(dba)_3{\cdot}CHCl_3$ (PPh_3/Pd = 2) in DMF containing nBu$_4$NBF$_4$ (0.3 M), two oxidation peaks were observed by cyclic voltammetry (Figure 2a): the minor peak at O_1 ($E^p = +0.10$ V vs SCE) characterizes $Pd^0(PPh_3)_2$,[6,13] and the major peak at O_2 characterizes the major complex Pd^0-(dba)$(PPh_3)_2$,[14] as already observed for the precursor $Pd^0(dba)_2$ (Scheme 2).[6,8,14] When PPh_3 was added to Pd^0_2(dba-4,4′-F)$_3$ (PPh_3/Pd = 2), two oxidation peaks were detected by cyclic voltammetry (Figure 2c). The minor peak appeared at the same potential O_1 as for $Pd^0(PPh_3)_2$ (Figure 2a); the major peak at O'_2 characterizes the major complex Pd^0(dba-4,4′-F)$(PPh_3)_2$ (Figure 2c, first equation in Scheme 6), which is less easily oxidized than $Pd^0(dba)(PPh_3)_2$ due to the electron-withdrawing effect of the two fluorine atoms (Table 1, entries 4 and 5). The oxidation peak current of $Pd^0(PPh_3)_2$ at O_1 increased at the expense of O'_2 upon addition of excess PPh_3, resulting in formation of $Pd^0(PPh_3)_3$ (Figure 2d, second equation in Scheme 6), as also observed for the simple nonsubstituted dba ligand (Figure 2b). Due to the fast equilibrium between $Pd^0(PPh_3)_3$, $Pd^0(PPh_3)_2$, and PPh_3 (Scheme 6), a single oxidation peak was observed at O_1.[6]

Scheme 6

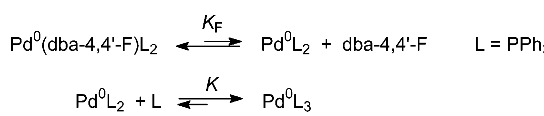

After addition of PhI (10 equiv), the oxidation peaks of Pd^0-(η^2-dba-4,4′-F)$(PPh_3)_2$ and $Pd^0(PPh_3)_2$, disappeared, attesting to

(12) Amatore, C.; Carré, E.; Jutand, A. *Acta Chem. Scand*. **1998**, *52*, 100−106.

(13) $Pd^0(PPh_3)_2$ is probably coordinated by the solvent (DMF), which is omitted for clarity.

(14) (a) The oxidation potential of $Pd^0(dba)(PPh_3)_2$ generated from Pd^0_2-(dba)$_3$ is slightly less positive than when it is generated from $Pd^0(dba)_2$ (entry 5 in Table 1). This is due to their respective equilibria with Pd^0-$(PPh_3)_2$ and dba, which is affected by the dba concentration (CE mechanism).[15] (b) The oxidation peak currents of $Pd^0(dba)(PPh_3)_2$ and $Pd^0(PPh_3)_2$ do not reflect the thermodynamic concentrations of the two complexes but their dynamic concentrations. Indeed, the oxidation of $Pd^0(PPh_3)_2$ at the electrode (at O_1) causes a continuous shift of the equilibrium in Scheme 2 toward its right-hand side. Under these conditions, the concentration of Pd^0-$(PPh_3)_2$ measured by its oxidation peak current is higher than its thermodynamic concentration in the equilibrium of Scheme 2 (CE mechanism).[15]

an oxidative addition leading to *trans*-$PhPdI(PPh_3)_2$. A new oxidation peak appeared at +0.540 V, which characterized the iodide ions released in the equilibrium between *trans*-$PhPdI(PPh_3)_2$ and the cationic complex *trans*-$[PhPd(PPh_3)_2(DMF)]^+$ (Scheme 5).[12]

The cyclic voltammetric and ^{31}P NMR spectroscopic data of other complexes $Pd^0(\eta^2$-dba-*n,n′*-Z$)(PPh_3)_2$ are listed in Table 1. As expected, $Pd^0(\eta^2$-dba-*n,n′*-Z$)(PPh_3)_2$ complexes are less and less easily oxidized when Z becomes more electron accepting, an outcome explained by Pd(0) becoming less and less electron rich. The cyclic voltammograms exhibited the minor common complex $Pd^0(PPh_3)_2$, which was generated in an unfavorable equilibrium with Pd^0(dba-*n,n′*-Z)$(PPh_3)_2$ and dba-*n,n′*-Z, as observed for the nonsubstituted dba (Scheme 2).[6]

Role of dba-*n,n′*-Z in the Kinetics of the Oxidative Addition of PhI with the Pd^0 Complexes Generated from Pd^0_2(dba-*n,n′*-Z)$_3$ and PPh_3 in DMF. The oxidative addition reactions were performed in DMF at 20 °C from PhI (2 mM) and Pd^0_2(dba-4,4′-F)$_3$ (1 mM) associated with PPh_3/Pd = 2, 4. Accurate kinetics were monitored by amperometry performed at a rotating-gold-disk electrode, polarized on the oxidation wave of $Pd^0(PPh_3)_2$.[6,16] After addition of PhI, the decrease of the oxidation current of $Pd^0(PPh_3)_2$ (proportional to is concentration)[6] was recorded versus time until total conversion (Figure 3a for 4,4′-F). The kinetics were compared to those for the reaction of PhI (2 mM) with $Pd^0_2(dba)_3$ (1 mM) associated with 2 equiv of PPh_3 per Pd (Figure 3a). The half-reaction times are given in Table 2. By a comparison of the three kinetic curves of Figure 3a (or the half-reaction times $t_{1/2}$ given in entries 2 and 3 in Table 2), the following reactivity orders were established:

$$^1/_2Pd^0_2(\text{dba-4,4'-Z})_3 + 2PPh_3 < {}^1/_2Pd^0_2(\text{dba})_3 + 2PPh_3$$

$$^1/_2Pd^0_2(\text{dba-4,4'-Z})_3 + 4PPh_3 < {}^1/_2Pd^0_2(\text{dba-4,4'-Z})_3 + 2PPh_3$$

This is in agreement with the mechanism of Scheme 7, already established for $Pd^0(dba)_2$.[6,8] The kinetic law was solved for the system $\{^1/_2Pd^0_2(\text{dba-4,4'-Z})_3 + 2PPh_3\}$ (Scheme 8).[17]Taking into account the variation of dba-4,4′-Z concentration during the reaction and the stoichiometry PhI/Pd^0 = 1, the kinetic law is expressed as in eq 1, where x is the molar fraction of $Pd^0(PPh_3)_2$

$$\ln x + 1.5/x = K_Z kt + 1.5 \qquad (1)$$

($x = i/i_0$, i = oxidation current of $Pd^0(PPh_3)_2$ at t, i_0 = initial oxidation current of $Pd^0(PPh_3)_2$).[17] The plot of $\ln x + 1.5/x$ against time was linear (Figure 3b for *n,n′*-Z = 4,4′-F) in agreement with eq 1, confirming a first-order reaction for PhI and the Pd^0 complex. The value of K_Zk was determined from the slope (Table 2).

The kinetics of the oxidative addition were similarly investigated for dba-4,4′-OMe and dba-3,3′,4,4′,5,5′-OMe (entries 1−4 in Table 2). By comparing the values of K_Zk which characterized the reactivity of the Pd^0 complexes generated from

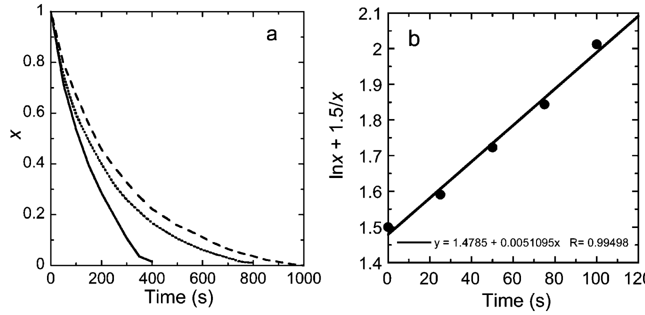

Figure 3. (a) Kinetics of the oxidative addition of PhI (2 mM) to the $Pd^0(PPh_3)_2$ complex generated from (—) $Pd^0_2(dba)_3$ (1 mM) + PPh_3 (4 mM); (···) Pd^0_2(dba-4,4′-F)$_3$ (1 mM) + PPh_3 (4 mM), and (-- -) Pd^0_2(dba-4,4′-F)$_3$ (1 mM) + PPh_3 (8 mM) in DMF at 20 °C. Plot of the molar fraction x of $Pd^0(PPh_3)_2$ ($x = i/i_0$, i = oxidation current of $Pd^0(PPh_3)_2$ at t, i_0 = initial oxidation current of $Pd^0(PPh_3)_2$). (b) Kinetics of the oxidative addition of PhI (2 mM) to the $Pd^0(PPh_3)_2$ complex generated from Pd^0_2(dba-4,4′-F)$_3$ (1 mM) + PPh_3 (4 mM) in DMF at 20 °C. Plot of $\ln x + 1.5/x$ versus time (x was determined from Figure 3a).

Table 2. Comparative Reactivity of Pd^0 Complexes Generated from Pd^0_2(dba-4,4′-Z)$_3$ (1 mM) Associated to 2 PPh_3/Pd or 4 PPh_3/Pd or from Pd^0(dba-4,4′-Z)$_2$ (2 mM) Associated to 4 PPh_3/Pd in the Oxidative Addition with PhI (2 mM) in DMF (20 °C)[a]

	n,n′-Z	$t_{1/2}$ (s) 2 PPh_3/Pd^0	$t_{1/2}$ (s) 4 PPh_3/Pd^0	10^3K_Zk (s^{-1})
	Pd^0_2(dba-4,4′-Z)$_3$			
1	4,4′-OMe	40	80	20
2	4,4′−H	115	130	7.0
3	4,4′−F	150	180	5.1
4	3,3′,4,4′,5,5′-OMe	65	125	12
	Pd^0(dba-4,4′-Z)$_2$			
5	4,4′-Me		125	
6	4,4′−H		150	
7	4,4′-Cl		345	
8	4,4′-Br		412	
9	3,3′,5,5′-OMe		198	

[a] $t_{1/2}$ = half-reaction time. See Schemes 7 and 8 for the mechanism and the definition of K_Z and k.

Scheme 7

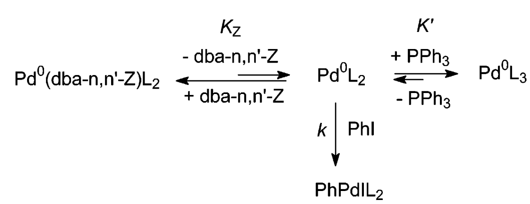

Scheme 8

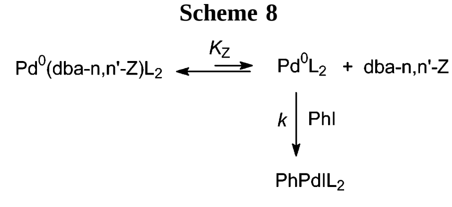

Pd^0_2(dba-4,4′-Z)$_3$, one deduces the following order of reactivity:

$$\text{4,4'-OMe} > \text{4,4'-H} > \text{4,4'-F}$$

When the Pd^0 precursor Pd^0_2(dba-4,4′-Z)$_3$ is ligated by a dba substituted by two electron-donating groups Z in the para position, the resulting system is more reactive in oxidative addition than when it is substituted by electron-withdrawing groups. Since the same reactive $Pd^0(PPh_3)_2$ species is involved

(15) Bard, A. J.; Faulkner, L. R. *Electrochemical Methods*, 2nd ed.; Wiley: New York, 2001.

(16) Due to the partial release of iodide ions in the oxidative addition which are oxidized at +0.54 V, it was not possible to investigate the kinetics of the oxidative addition upon polarizing the electrode at the oxidation potential of Pd^0(dba-4,4′-Z)$(PPh_3)_2$.

(17) $d([Pd^0])/dt = -k[PhI][Pd^0]/([\text{dba-4,4'-H}]/K_Z + 1)$; $d([Pd^0])/[Pd^0] = -k[PhI]dt/([\text{dba-4,4'-H}]/K_Z + 1)$ with $[Pd^0] = C_0x$; $[PhI] = C_0x$ and $[\text{dba-4,4'-H}] = C_0(1.5 - x)$. Since $C_0/K_Z \gg 1$, one gets $(1.5 - x)dx/x^2 = -kK_Zdt$, which gives eq 1 after integration (see text).

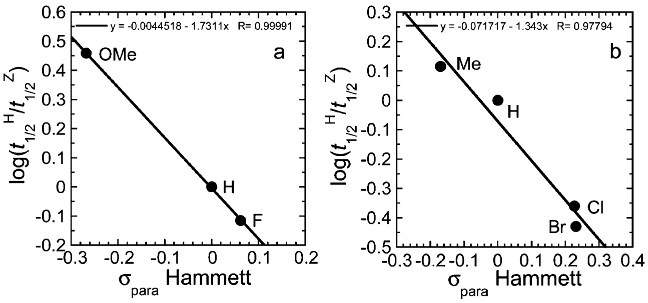

Figure 4. (a) Hammett plot for the oxidative addition of PhI (2 mM) with the $Pd^0(PPh_3)_2$ complex generated from (a) Pd^0_2(dba-4,4′-Z)$_3$ (1 mM) and PPh_3 (4 mM) in DMF at 20 °C and (b) Pd^0-(dba-4,4′-Z)$_2$ (2 mM) and PPh_3 (8 mM) in DMF at 20 °C.

(Scheme 8), this means that its concentration decreases when going from Z = OMe to Z = F. In other words, K_Z must decrease when going from Z = OMe to Z = F. The rate constant k does not depend on Z; only the equilibrium constant K_Z is affected by Z. From the values of K_Zk given in Table 2 (entries 1−3), one concludes that indeed

$$K_{4,4'-\mathrm{OMe}} > K_{4,4'-\mathrm{H}} > K_{4,4'-\mathrm{F}}$$

The $Pd^0(PPh_3)_2$ concentration decreases when going from Z = OMe to Z = F because dba-4,4′-Z becomes an increasingly better ligand (more electron deficient) for the electron-rich Pd^0-(PPh_3)$_2$ species. Only three substituents in the para position have been investigated here, although their electronic properties can be considered distinct. A Hammett plot was nevertheless tested (Figure 4a). The kinetics of the overall oxidative addition obey a Hammett plot with a negative slope ($\rho = -1.7$). The reactivity of the Pd^0 complex generated from Pd^0_2(dba-4,4′-CF_3)$_3$ associated with 2 or 4 equiv of PPh_3 per Pd center could not be investigated, because the oxidation peak of $Pd^0(PPh_3)_2$ was not detected by cyclic voltammetry, due its overly low concentration in its equilibrium with Pd^0(dba-4,4′-CF_3)(PPh_3)$_2$.[16]

One also observes the following reactivity order (Table 2, entries 1 and 4):

$$\text{4,4'-OMe} > \text{3,3',4,4',5,5'-OMe}$$

This means that Pd^0(dba-3,3′,4,4′,5,5′-OMe)(PPh_3)$_2$ is less dissociated to $Pd^0(PPh_3)_2$ than Pd^0(dba-4,4′-OMe)(PPh_3)$_2$, which could be explained by competing donating/withdrawing effects in the para and meta positions, in the case of the dba-3,3′,4,4′,5,5′-OMe ligand, for which the individual electronic contributions cannot be easily deconstructed.

Role of dba-*n*,*n*′-Z in the Kinetics of the Oxidative Addition of PhI with the Pd^0 Complexes Generated from Pd^0(dba-*n*,*n*′-Z)$_2$ and PPh_3 in DMF. The Pd^0 complexes ligated to dba-4,4′-Z (Z = Me, Br, Cl) were more stable when isolated as Pd^0(Z-dba)$_2$.[11] The oxidative addition of PhI (2 mM) to Pd^0(dba-4,4′-Z)$_2$ (2 mM) associated to PPh_3 (8 mM) (PPh_3/Pd^0 = 4) was investigated as above in DMF at 20 °C. For the same initial concentration C_0 of Pd^0(dba-4,4′-Z)(PPh_3)$_2$, the amount of $Pd^0(PPh_3)_2$ is lower when starting from Pd^0(dba-4,4′-Z)$_2$ than from Pd^0_2(dba-4,4′-Z)$_3$, due to the higher initial dba-4,4′-Z concentration in the former precursor (C_0) than in the latter one (C_0/2). The ratio $PPh_3/Pd^0 = 4$ was thus selected to facilitate the detection of $Pd^0(PPh_3)_2$ by amperometry at the rotating disk electrode. The mechanistic scheme is given in Scheme 7. The values of the half-reaction times, $t_{1/2}$, are given in Table 2 (entries 5−9). As predicted above, we observe that the Pd^0 complex generated from Pd^0(dba-4,4′-H)$_2$ (Table 2, entry 6, $t_{1/2}$ = 150 s) is less reactive than the Pd^0 complex generated from Pd^0_2(dba-4,4′-H)$_3$ (Table 2, entry 2, $t_{1/2}$ = 130 s) in oxidative additions performed at identical concentrations (Pd^0/PPh_3/PhI = 1/4/1, C_0 = 2 mM), due to the higher initial concentration of the free dba in the former system.

$$Pd^0(dba)_2 + 4PPh_3 < {}^1/_2Pd^0{}_2(dba)_3 + 4PPh_3$$

By now considering Pd^0(dba-*n*,*n*′-Z)$_2$ precursors associated with 4 equiv of PPh_3 and comparing the values of the half-reaction times $t_{1/2}$ (Table 2, entries 5−8), the following reactivity order is observed:

$$\text{4,4'-Me} > \text{4,4'-H} > \text{4,4'-Cl} > \text{4,4'-Br}$$

This establishes that, in association with PPh_3, the Pd^0 precursor Pd^0(dba-4,4′-Z)$_2$ ligated by a dba substituted by two electron-donating groups Z in the para position gives rise to a more reactive system in oxidative addition as compared to the case when it is substituted by two electron-withdrawing groups, as observed above starting from Pd^0_2(dba-4,4′-Z)$_3$. The equilibrium constant K' and the rate constant k (Scheme 7) are not dependent on the structure of Z. Consequently, one finds

$$K_{4,4'-\mathrm{Me}} > K_{4,4'-\mathrm{H}} > K_{4,4'-\mathrm{Cl}} > K_{4,4'-\mathrm{Br}}$$

The overall oxidative addition process follows a Hammett plot with a negative slope ($\rho = -1.3$) (Figure 4b), as found for the precursor Pd^0_2(dba-4,4′-Z)$_3$ (Figure 4a).[18]

Conclusion

The ligand dba-*n*,*n*′-Z plays a crucial role in the kinetics of oxidative additions by controlling the concentration of the active $Pd^0(PPh_3)_2$ via its equilibrium with Pd^0(dba-4,4′-Z)(PPh_3)$_2$ (equilibrium constant K_Z). As a result, the more electron donating the Z group, the higher the K_Z value and consequently the faster the rate of the overall oxidative addition. The complex Pd^0(dba-4,4′-Z)(PPh_3)$_2$ is more dissociated to $Pd^0(PPh_3)_2$ when Z is an electron-donating group, because the affinity of dba substituted by an electron-donating group, for the electron-rich $Pd^0(PPh_3)_2$ species, is less than that of dba substituted by an electron-accepting group. It is then possible to increase the reactivity of the palladium(0) complexes in the oxidative addition process by changing the dba structure (substitution by an electron-donating group Z) of the catalytic precursor and also by using $Pd^0_2(dba)_3$ instead of $Pd^0(dba)_2$. The increased catalytic activity observed by Fairlamb et al.[10] with Z = OMe in Suzuki−Miyaura reactions involving poorly reactive aryl chlorides is then rationalized by a faster oxidative addition step.

Experimental Section

General Methods. All experiments were performed using standard Schlenk techniques under an argon atmosphere. The ^{31}P NMR spectra were recorded on a Bruker spectrometer (101 MHz) using H_3PO_4 as an external reference; the ^{19}F NMR spectra were recorded on a Bruker spectrometer (235 MHz) with $CFCl_3$ as an

(18) Despite the accelerating effect found for the Pd(0) complex generated from Pd^0(dba-4,4′-Br)$_2$ when compared to the case for $Pd^0(dba)_2$, no competitive oxidative addition proceeded with the 4-bromobenzylidene ligand. Indeed, the ^{31}P NMR spectrum of Pd^0(dba-4,4′-Br)(PPh_3)$_2$ generated after addition of 2 PPh_3 to Pd^0(dba-4,4′-Br)$_2$ in DMF or toluene displayed the two doublets of Pd^0(dba-4,4′-Br)(PPh_3)$_2$ without any additional signals which would have characterized an (aryl)Pd^{II}Br(PPh_3)$_2$ complex formed in the oxidative addition of the 4-bromobenzylidene ligand with the Pd(0) complex. Moreover, the free dba-4,4′-Br ligand was fully recovered by chromatography after the NMR sample had decomposed (to give Pd black).

external reference. Cyclic voltammetry and amperometry were performed using an in-house-constructed potentiostat and a GSTP4 waveform generator (Radiometer Analytical). The current was recorded on a Nicolet 301 oscilloscope.

Chemicals. DMF was distilled from CaH_2 and kept under argon. PPh_3 and phenyl iodide were obtained from a commercial source (Aldrich). The precursors Pd^0_2(dba-*n*,*n*′-Z)$_3$ (*n*,*n*′-Z = 4,4′-F, 4,4′-H, 4,4′-MeO, 3,3′,4,4′,5,5′-OMe) and Pd^0(dba-*n*,*n*′-Z)$_2$ (*n*,*n*′-Z = 4,4′-CF_3, 4,4′-Me, 4,4′-Br, 4,4′-Cl, 4,4′-H, 3,3′,5,5′-OMe) were synthesized according to published procedures.[10,11]

General Procedure for ^{31}P and ^{19}F NMR Experiments. To 0.75 mL of degassed DMF was introduced 13 μmol of Pd^0(dba-*n*,*n*′-Z)$_2$ or 6.5 μmol of Pd^0_2(dba-*n*,*n*′-Z)$_3$ followed by 6.8 mg (26 μmol) of PPh_3. A 75 μL portion of degassed acetone-d_6 was then added for the lock.

General Procedure for the Cyclic Voltammetry and for the Kinetics of the Oxidative Addition Followed by Amperometry. Experiments were carried out in a three-electrode thermostated cell connected to a Schlenk line. The reference was a saturated calomel electrode (Radiometer) separated from the solution by a bridge filled with 3 mL of a 0.3 M $n$$Bu_4NBF_4$ solution in DMF. The counter electrode was a platinum wire of ca. 1 cm^2 apparent surface area. A 15 mL portion of DMF containing $n$$Bu_4NBF_4$ (0.3 M) was poured into a cell. A 15 μmol portion (1 mM) of Pd^0_2(dba-*n*,*n*′-Z)$_3$ (*n*,*n*′-Z = 4,4′-F, 4,4′-H, 4,4′-MeO, 3,3′,4,4′,5,5′-OMe) or 30 μmol (2 mM) of Pd^0(dba-*n*,*n*′-Z)$_2$ (*n*,*n*′-Z = 4,4′-Me; 4,4′-Br;, 4,4′-Cl;, 4,4′-H, 3,3′,5,5′-OMe) was then introduced into the cell followed by 15.7 mg (60 μmol, 4 mM) or 31.4 mg (120 μmol, 8 mM) of PPh_3. The cyclic voltammetry was performed at a stationary-gold-disk electrode (diameter 2 mm) at a scan rate of 0.5 V s^{-1}.

The kinetic measurements were performed at a rotating-gold-disk electrode (diameter 2 mm, inserted into a Teflon holder, EDI 65109, Radiometer) with an angular velocity of 105 rad s^{-1} (Radiometer). The rotating electrode was polarized at +0.2 V on the plateau of the oxidation wave of $Pd^0(PPh_3)_2$. A 3.3 μL portion (30 μmol, 2 mM) of phenyl iodide was then added to the cell and the decay of the oxidation current recorded versus time up to 100% conversion at 20 °C.

Acknowledgment. This work was supported in part by the Centre National de la Recherche Scientifique (UMR CNRS-ENS-UPMC 8640) and the Ministère de la Recherche (Ecole Normale Supérieure). We thank Johnson Matthey for a generous loan of palladium salts (A.J. and I.J.S.F.). We are also grateful to the Royal Society for funding a university research fellowship and for providing a generous equipment grant (to I.J.S.F.).

OM0510876